

Layered tungsten oxide-based organic/inorganic hybrid materials I: Infrared and Raman study

B. Ingham

Victoria University of Wellington, P.O. Box 600, Wellington, New Zealand

S.V. Chong and J.L. Tallon

Industrial Research Ltd., P.O. Box 31310, Lower Hutt, New Zealand.

(Dated: October 25, 2018)

Tungsten oxide-organic layered hybrid materials have been studied by infrared and Raman spectroscopy, and demonstrate a difference in bonding nature as the length of the interlayer organic ‘spacer’ molecule is increased. Ethylenediamine-tungsten oxide clearly displays a lack of terminal $-\text{NH}_3^+$ ammonium groups which appear in hybrids with longer alkane molecules, thus indicating that the longer chains are bound by electrostatic interactions as well as or in place of the hydrogen bonding that must be present in the shorter chain ethylenediamine hybrids. The presence of organic molecules between the tungsten oxide layers, compared with the layered tungstic acid H_2WO_4 , shows a decrease in the apical $\text{W}=\text{O}$ bond strength, as might be expected from the aforementioned electrostatic interaction.

INTRODUCTION

Layered transition metal oxides present a paradigm for strongly correlated electronic systems subject to interesting correlated states and the competition of multiple order parameters. The high temperature oxide superconductors are a much-studied case in point. Moreover the discovery of superconductivity in sodium cobalt oxide [1] confirms this general approach of exploring novel layered metal oxides. Here we consider layered tungstates as another new model system capable of displaying a complex phase behaviour dependent upon interlayer coupling and doping state.

Tungsten oxide has been the subject of much research in the past few decades due to its interesting physical and electronic properties and doping capability. Tungsten trioxide can form a variety of stable structures at room temperature, such as pyrochlore, hexagonal, or distorted cubic [2, 3, 4, 5], all of which are comprised of corner- and/or edge-shared WO_6 octahedra. These structures can be doped by inserting mono- or di-valent atomic species into the interstitial vacancy sites within the oxide structure [5, 6, 7, 8], or by removing oxygen [9, 10, 11]. This results in an increase in electrical conductivity [12, 13, 14, 15] and dramatic colour changes [10, 12, 16], which has led to tungsten trioxide systems being used in electrochromic applications [17, 18, 19].

Tungsten trioxide can be hydrated to form layered structures, with a general formula of $\text{WO}_3 \cdot x\text{H}_2\text{O}$. In the mono-hydrate, $\text{WO}_3 \cdot \text{H}_2\text{O}$ (or H_2WO_4), two-dimensional layers of corner-shared WO_6 octahedra are formed, with a water molecule ($-\text{OH}_2$) substituted for one apical oxygen of the tungsten atom, and a terminal oxygen completing the structure [20]. In the di-hydrate ($\text{WO}_3 \cdot 2\text{H}_2\text{O}$), the second water molecule is inserted between the layers, as in $\text{MoO}_3 \cdot 2\text{H}_2\text{O}$ [21]. An increase in the interlayer spacing is observed [22] and it thus follows that

one could perhaps substitute organic species between the tungsten oxide layers. Indeed this has proven successful, with various groups succeeding in intercalating organic molecules such as pyrazine [23], 4,4-bipyridine [23, 24], pyridine [24], tert-alkylammonium species [25], mono-aminoalkanes [26] and diamino-alkanes [27]. Such materials provide an interesting template for doping and substitutional (e.g. magnetic ions) studies in low-dimensional systems.

Here we present infrared and Raman results on a selection of WO_3 -based hybrid materials in order to gain a more extensive understanding of the overall structure; in particular, the bonding nature of the organic to the inorganic layer, and the impact of the organic intercalant on the structure of the inorganic layer.

EXPERIMENTAL

Diaminoalkane-tungsten oxide samples were synthesised as described in Ref. 28. In brief, H_2WO_4 was dissolved in hot aqueous ammonia solution (33 wt. %) and then a solution of the organic amines (α,ω -diamine, $\text{H}_2\text{N}(\text{CH}_2)_n\text{NH}_2$, hereby abbreviated to DAN; or phenethylamine, $\text{C}_6\text{H}_5(\text{CH}_2)_2\text{NH}_2$, abbreviated to phen) dissolved in ammonia was added in a 2:1 molar ratio. The excess solvent was then evaporated off and the hybrid materials were obtained as white/cream-coloured powders. The entire synthesis was carried out under flowing N_2 gas.

Powder X-ray diffraction spectra were recorded using a Philips PW1700 series powder diffractometer with $\text{Co K}\alpha$ radiation. Infrared spectra were collected on a Bomem DA8 FT spectrometer over the mid-IR range ($450\text{--}4000\text{ cm}^{-1}$) using the KBr disc method with a resolution of 2 cm^{-1} . Raman spectra were collected using a Jobin-Yvon LabRam HR spectrometer with an excitation wavelength

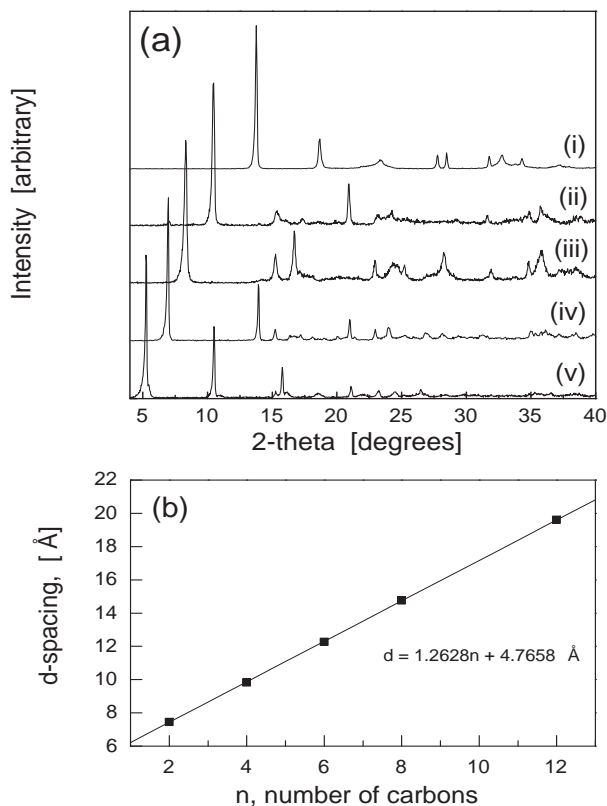


FIG. 1: (a) X-ray diffraction spectra of tungsten oxide-based hybrid materials: (i) W-DA2; (ii) W-DA4; (iii) W-DA6; (iv) W-DA8; (v) W-DA12. (b) Linear progression of first major peak versus alkane chain length.

of 633 nm.

RESULTS AND DISCUSSION

The X-ray diffraction spectra shown in Figure 1a display a strong peak at low 2θ angles. As the length of the intercalated organic molecule is increased, the corresponding d-spacing also increases in a linear fashion (shown in Figure 1b). From the slope and intercept of this line we propose a model by which single molecular layers of 2-dimensional corner-shared WO_6 octahedra are separated by the organic molecules which are aligned almost perpendicular to the tungsten oxide layers. One would expect such a layered compound to display properties approaching those of a purely 2-dimensional system as the distance between the oxide layers is increased (by increasing the length of the organic spacer molecule). The physical properties of this system will be the topic of future publications.

The normalised infrared and Raman spectra of the solid samples studied are shown in Figures 2-4, and the peak positions tabulated in Tables I-II. The di-

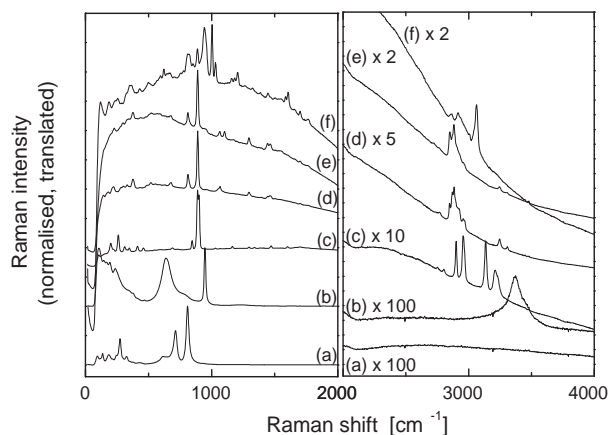


FIG. 2: Raman spectra of tungsten oxide-related materials: (a) WO_3 ; (b) H_2WO_4 ; (c) W-DA2; (d) W-DA6; (e) W-DA12; (f) W-phen. The high frequency region is displayed on a different scale to enable the important features to be seen.

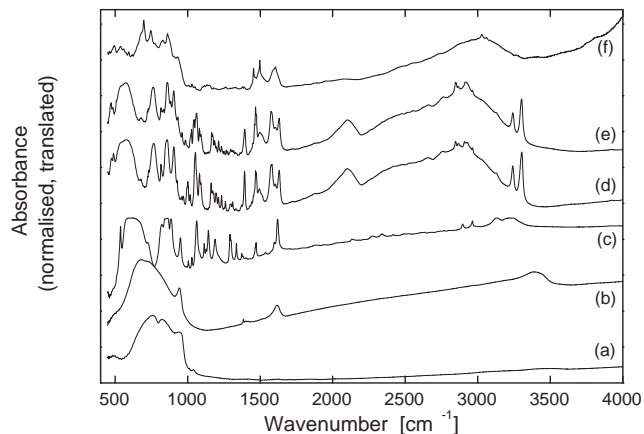


FIG. 3: Infrared spectra of tungsten oxide-related materials: (a) WO_3 ; (b) H_2WO_4 ; (c) W-DA2; (d) W-DA6; (e) W-DA12; (f) W-phen.

aminoalkane hybrids $\text{WO}_4 \cdot \text{DAn}$ (hereby abbreviated to W-DAn) with alkyl lengths longer than two carbons have virtually identical spectra [27, 28] and so are summarised in the tables as W-DAn, in comparison with the differing W-DA2.

The infrared spectra of WO_3 and its hydrate, H_2WO_4 , have much fewer and broader peaks than their hybrid counterparts. Both the infrared and Raman spectra of these two compounds correspond well with those presented by Daniel et al. [22]. These results are summarised in three sections: the effect on the inorganic layer, the effect on the organic species, and the organic-inorganic bonding nature.

TABLE I: Observed peaks in powder samples, 1000-4000 cm^{-1} . ν stretching, δ deformation/in-plane bending, *sciss.* scissoring, σ bending, ω wagging; *s* strong, *m* medium, *w* weak, *vw* very weak, *b* broad.

Assignment	WO ₃		H ₂ WO ₄		W-DA2		W-DAn		W-phen	
	IR	Raman	IR	Raman	IR	Raman	IR	Raman	IR	Raman
$\nu(\text{O-H})$			3410 mb	3370 w						
							3302 s	3305 vw		
					3244 wb		3242 m	3247 w		
$\nu(\text{NH}_2, \text{NH}_3^+)$					3212 wb	3212 m				
					3134 wb	3135 s				
									3061 w	3063 m
									3028 w	
									3006 w	
$\nu(\text{CH}_2)$					2963 w	2956 s	2963 w	2960 w		
					2895 w	2900 s	2919 w	2924 w		2916 w
							2910 w	2883 m		
							2868 w	2870 m		2861 w
							2847 w	2849w		
$\delta(\text{NH}_3^+)$							2101 mb		2090 vw	
Organic							1762 vw		1760 vw	1766 w
							1700 vw		1701 vw	1702 w
$\delta(\text{H}_2\text{O})$			1614 m							
$\delta(\text{NH}_2/\text{NH}_3^+)$					1620 s		1631 s			
					1597 w	1602 vw	1604 w		1605 mb	1606 w
							1578 s		1591 mb	1586 w
Sciss. CH ₂					1471 m	1472 w	1495 m		1497 ^a m	1500 ^a vw
					1467 w		1469 s	1465 w		
							1445 vw	1444 w	1454 ^a m	1446 ^a w
Sciss. and $\sigma(\text{CH}_2)$					1403 vw	1412 vw				
					1382 vw	1386 vw	1393 s		1384 vw	1386 vw
					1373 w					
$\sigma(\text{CH}_2), \omega(\text{CH}_2)$					1336 m	1340 vw	1310 w		1333 vw	1322 vw
					1299 m	1296 vw	1298 w	1296 w		
							1292 m		1261 vw	1266 vw
										1206 m
$\sigma(\text{NH}_2, \text{NH}_3^+)$					1189 m		1197 w			
							1173 m		1181 vw	1183 w
					1144 m	1164 vw	1164 m		1152 vw	1161 w
					1128 vw				1132 vw	
					1114w					
$\nu(\text{C-N}, \text{C-C})$								1103 w		
					1062 s	1070 vw	1083 m	1066 w		
							1059 s			
					1030 w	1030 vw	1027 m			1030 m
					1006 w		1001 m			
							962 w	953 vw	929 mb	942 sb

^aAromatic C=C stretch.

TABLE II: Observed peaks in powder samples, 0-1000 cm^{-1} . ν stretching, δ deformation/in-plane bending, ρ rocking; s strong, m medium, w weak, vw very weak, b broad.

Assignment	WO_3		H_2WO_4		W-DA2		W-DAn		W-phen	
	IR	Raman	IR	Raman	IR	Raman	IR	Raman	IR	Raman
$\nu(\text{W}=\text{O})$	940 mb	940 vw	950 s	947 s	951? m	900 s				
					885 s	888 s	905 s	890 s	902 wb	1004? s
					857 sb		859 s		861 s	888 m
					841 sb	846 m				854 m
$\nu(\text{O}-\text{W}-\text{O})$	824 sb	809 s			822 mb		816 m	813 m	829 m	816 mb
	756 sb			774 mb			760 ^b sb		775 ^b mb	
		714 m	740 sb		724 mb	732 vw			745 s	
			680 sb		674 sb	690 w	678 vw	679 w	697 s	668 w
		614 w		638 sb	613 sb					622 m
						594 vw	577 sb	576 vw	594 vw	595 w
Organic					537 s	550 vw	545 sb	552 vw	557 w	
							487 w	490 vw	495 w	502 m
						460 w	474 w			
Inorganic		434 vw		467 vw		412 w		436 vw		432 w
W-OH ₂				377 vw				377 m		362 mb
$\delta(\text{O}-\text{W}-\text{O})$		326 w		330 vw		348 w		336 vw		
		274 m				311 w		301 vw		
						261 m		283 vw		
$\nu(\text{W}-\text{O}-\text{W})$		252 w		236 w		222 w		226 w		254 w
										238 w
Lattice modes		187 w		194 w		201 m		182 vw		187 w
		136 w		144 vw				144 vw		120 vw
		94 w		106 w						

^b $\rho(\text{NH}_3^+)$ mode.

I. The effect on the inorganic layer

The presence of co-ordinated water molecules in H_2WO_4 can be seen by the broad O-H stretching peak at 3410 (3370) cm^{-1} (IR and Raman respectively), the H_2O bending peak at 1614 cm^{-1} (IR only), and the W-OH₂ co-ordinated water peak in the Raman spectrum at 377 cm^{-1} . These peaks do not occur in the WO_3 spectra, as expected.

As mentioned earlier, the structure of H_2WO_4 consists of layers of corner-shared WO_6 octahedra with alternate apical arrangements of W-OH₂ and W=O. In the Raman spectrum the W=O bonding is shown clearly by a sharp band centred at about 950 cm^{-1} . This is also present in the IR spectrum. Surprisingly, the WO_3 sample also exhibits a small peak at this position in the Raman and IR spectra. This is not expected as the structure of WO_3 consists only of single W-O bonds. However it can be explained by the presence of disorder in the sample and loss of oxygen [29][41], which results in the formation of a small fraction of W=O bonds. There are also W=O

terminations on the surfaces of the powder particles.

In the diaminoalkane hybrid compounds the characteristic W=O peak, formerly at 950 cm^{-1} in H_2WO_4 , shifts to a lower frequency of 890-900 cm^{-1} . While in several of these compounds there are peaks at 950 cm^{-1} they are not as intense as the W=O peak. It is also of interest to note that the peak at 888 cm^{-1} in the W-DA2 Raman spectrum is a doublet, suggesting perhaps the presence of two different W=O bonds. In W-phen, the peak structure in the range 900-100 cm^{-1} is quite different from the other hybrid spectra. This may be due to the organic molecule being mono-dentate (as IR spectra of other mono-aminoalkane hybrids show that the 950 cm^{-1} W=O peak is virtually unaltered [30]) or more complicated due to the presence of the aromatic ring. In any case, the sharp Raman peak at 1004 cm^{-1} is likely to be a W=O peak due to the similarity in shape between it and the known W=O peak in H_2WO_4 , for example. There may be more than one variation of the W=O bond within the structure, which may also account for the multiple peaks observed in this region, as is the

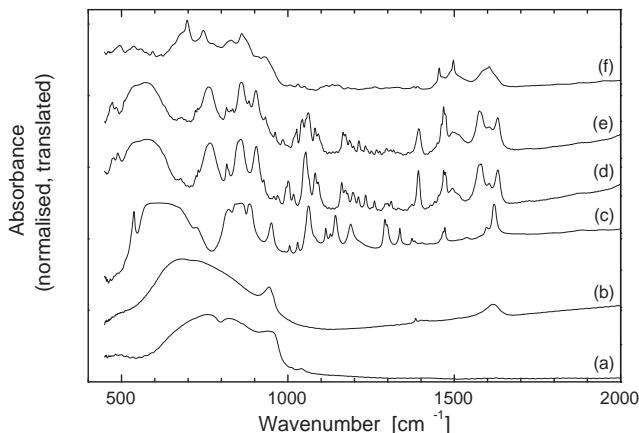


FIG. 4: Low-frequency region of the infrared spectra of tungsten oxide-related materials: (a) WO_3 ; (b) H_2WO_4 ; (c) W-DA2; (d) W-DA6; (e) W-DA12; (f) W-phen.

case in $\text{WO}_3 \cdot 2\text{H}_2\text{O}$ [22]. There is a relationship between bond length (an indication of bond strength) and the frequency of the vibrational modes(s) for the terminal W–O bond, namely that as the bond length decreases, bond strength and frequency increases [22, 31]. It is not therefore impossible to observe more than one terminal W–O vibration.

The remaining bands can be assigned as follows: 580–860 cm^{-1} O–W–O stretching, 430–470 cm^{-1} inorganic Raman mode (W–O), 260–350 cm^{-1} O–W–O bending, 220–250 cm^{-1} W–O–W stretching, 90–200 cm^{-1} lattice modes. These bands occur at similar positions in the hybrid compounds.

II. The effect on the organic species

Perhaps the most telling difference between W-DA2 and W-DAn ($n > 2$) is the presence or absence of the broad peak centred at 2100 cm^{-1} in the IR spectra. This feature is due to a combination of the asymmetrical $-\text{NH}_3^+$ bending vibration and the torsional oscillation of the $-\text{NH}_3^+$ group [32]. Both $-\text{NH}_2$ scissoring and $-\text{NH}_3^+$ bending occurs in the region 1580–1630 cm^{-1} , however the latter displays three peaks (as seen in W-DAn) while the former yields only two (as in W-DA2). Lastly, the N–H stretching bands occur at slightly higher energies in W-DAn compared with W-DA2 (3240–3300 cm^{-1} , c.f. 3135–3250 cm^{-1}) and these peaks are also much sharper. However, an increase in alkyl chain length should have little effect on the N–H stretching frequency [33]. The observed differences are discussed in Section III.

The presence of broad vibrational bands in the W-DAn spectra in the range 2430–2790 cm^{-1} can be ascribed to NH_3^+ symmetrical stretching [32, 34] and often appear as a broad, ill-defined band under the C–H stretching

modes near 2800 cm^{-1} [35]. In H_2WO_4 a small peak is observed in the IR spectrum at 1614 cm^{-1} , which corresponds to H_2O bending. While the hybrid samples also exhibit peaks near this value (1600–1630 cm^{-1}), these peaks are sharp and well defined, and the vibrational band at 3400 cm^{-1} (indicative of O–H stretching) is absent. Thus we conclude that most of the co-ordinated water molecules (W–OH₂) have been dehydrogenated during the organic intercalation process (a small feature at 377 cm^{-1} in the Raman spectra may correspond to W–O–H). The peaks in the hybrid spectra in the range 1600–1630 cm^{-1} correspond instead to NH_2 or NH_3^+ bending.

As only the terminal amino/ammonium group is involved in interactions with the inorganic layer, it is no surprise that the bands corresponding to C–H, C–N and C–C vibrations remain virtually unchanged. The peaks in the hybrid spectra corresponding to these vibrations can be assigned as follows: 2850–2960 cm^{-1} C–H stretching, 1300–1500 cm^{-1} CH_2 wagging, bending, and scissoring; also C=C aromatic stretching for W-phen (1450–1500 cm^{-1}), 950–1100 cm^{-1} C–N and C–C stretching. From 460–550 cm^{-1} there are a small number of unassigned organic bands (including a sharp peak in the IR at 537 cm^{-1} for W-DA2, corresponding to the bending vibration of the NCCN backbone [36]).

III. The organic-inorganic bonding nature

The most noticeable difference among the hybrid samples is that W-DA2 shows quite a different bonding nature to the hybrids with longer organic chains: there is no evidence for the presence of ammonium ($-\text{NH}_3^+$) terminal groups in W-DA2. As mentioned previously, W-DA2 lacks a feature at 2100 cm^{-1} found in the other hybrid spectra that corresponds to deformations of terminal $-\text{NH}_3^+$. Combined with the presence of the $-\text{NH}_3^+$ rocking mode found at 770 cm^{-1} [34], this implies that some of the amine molecules in W-DAn appear as $\text{R}-\text{NH}_3^+ \cdots \text{O}-\text{W}$, while all those of W-DA2 appear as neutral $-\text{NH}_2$ species. This raises the question of how charge balance is achieved in W-DA2 and also whether hydrogen bonding is the exclusive mechanism of bonding, whereas in the longer organic molecule hybrids there is clearly an electrostatic component as well due to the presence of terminal ammonium groups. There are also differences in the N–H stretch region, suggesting changes in the bonding chemistry as one progresses from DA2 to longer DAn alkyl chains. As mentioned in Section II, the N–H stretching bands for W-DA2 appear at lower wavenumbers than for longer-chain W-DAn species. Hydrogen bonding (which holds the DA2 molecules in place between the layers) will cause these bands to shift to lower frequencies [32]. DA2 is the only case where the inductive effect on the terminal amine groups is known

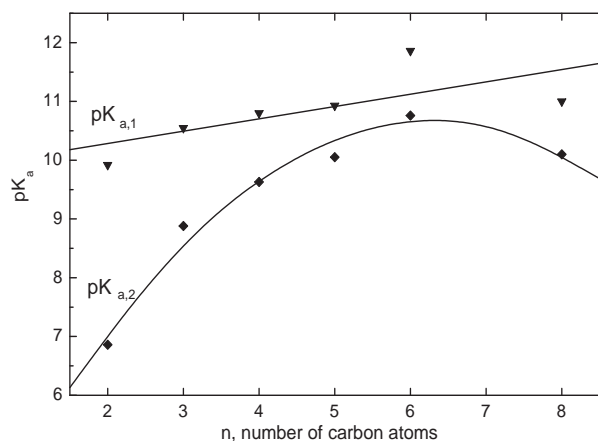


FIG. 5: Plot of pK_a values from Ref. 37 versus the number of carbon atoms of α,ω -diamines in aqueous solution.

to be a perturbing factor to the molecular vibrations due to the shorter alkyl chain length [33].

One possible explanation for the observed difference in structure between DA2 and longer DAN molecules intercalated into an acidic metal oxide, arises from examining the trend in basicity of α,ω -diamines in solution. Although the trend in basicity only changes slightly with increasing alkyl length for the monoamines (due to combinations of solution effect, steric hindrance to solvation, and number of available H-bonds [38, 39, 40]), a substantial increase in basicity is observed in going from DA2 to DA8 (Fig. 5). This increase in base strength for the diaminoalkanes is due to an increase of the inductive effect as the number of methylene groups ($-\text{CH}_2-$) increases. The formation of alkylammonium ($-\text{NH}_3^+$) end groups will therefore be more favourable for the more basic diaminoalkanes (i.e. diaminobutane and above). This apparent difference is also manifested in the TGA profile of these hybrids, with W-DA2 dissociating at a higher temperature than any of the other W-DAN compounds [27].

The strong Raman peak at 950 cm^{-1} in H_2WO_4 corresponds to an apical $\text{W}=\text{O}$ bond, which is characteristic of a layered structure. This peak is present in all of the hybrid compounds although it is shifted to lower wavenumbers of $890\text{--}900\text{ cm}^{-1}$, indicating that the apical oxygen is not as tightly bound to the tungsten as in H_2WO_4 . This too can be expected as charge balance in H_2WO_4 is achieved by co-ordinated water molecules binding alternately upper and lower of the tungsten layer, leaving the remaining apical oxygen atoms to bind relatively strongly. In the hybrid materials one might expect the influence of organic molecules on each apical oxygen to be more uniform, hence this interaction will weaken the $\text{W}=\text{O}$ bond, and this is indeed evident from the Raman shift. There is evidence to suggest that in W-phen, a monodentate amine hybrid, there are several variations

of the $\text{W}=\text{O}$ bond, which in itself warrants further study.

The structure and electronic density of states of these layered systems are currently being investigated by *ab initio* computations. The question of the relocation of protons in the W-DA2 system is a particular issue of study.

CONCLUSIONS

Infrared and Raman spectroscopy have been utilised to gain an understanding of the bonding nature between the organic and inorganic components of tungsten oxide-hybrid systems with different length diaminoalkanes and how the inclusion of organic molecules affects the structure of the inorganic layers. Tungsten oxide-ethylenediamine displays a different bonding nature from the other hybrid materials in that it appears to rely on hydrogen-bonding only, with no terminal $-\text{NH}_3^+$ ammonium groups to form electrostatic bonds. This is thought to be related to the lower basicity of ethylenediamine as opposed to the longer diaminoalkane species. All of the tungsten oxide-organic hybrid materials exhibit a decrease in the strength of the apical $\text{W}=\text{O}$ bond of the WO_4^{2-} layers compared with the layered tungsten oxide monohydrate (tungstic acid), H_2WO_4 .

ACKNOWLEDGMENTS

The authors would like to acknowledge the financial assistance from The New Zealand Foundation of Research Science and Technology (Contract number: IRLX0201), The Royal Society of New Zealand Marsden Fund, and The MacDiarmid Institute for Advanced Materials and Nanotechnology (Victoria University, New Zealand).

-
- [1] K. Takada, H. Sakurai, E. Takayama-Muromachi, F. Izumi, R. Dilanian, and T. Sasaki, *Nature* **422**, 53 (2003).
 - [2] B. Mourey, M. Hareng, B. Dumont, J. Desseine, and M. Figlarz, *Eurodisplay Proceedings* p. 223 (1984).
 - [3] J.-D. Guo, K. Reis, and M. Whittingham, *Solid State Ionics* **53**, 305 (1992).
 - [4] C. Genin, A. Driouiche, B. Gerand, and M. Figlarz, *Solid State Ionics* **53** (1992).
 - [5] J. Bailar, H. Emeleus, R. Nyholm, and A. Trotman-Dickenson, eds., *Comprehensive Inorganic Chemistry* (Pergamon, Oxford, 1973), vol. 4, chap. 50: Tungsten Bronzes, Vanadium Bronzes and Related Compounds.
 - [6] S. Haydon and D. Jefferson, *J. Solid State Chem.* **168**, 306 (2002).
 - [7] J. Bailar, H. Emeleus, R. Nyholm, and A. Trotman-Dickenson, eds., *Comprehensive Inorganic Chemistry* (Pergamon, Oxford, 1973), vol. 4, chap. 36: Chromium, Molybdenum and Tungsten.

- [8] C. Grenthe and M. Sundberg, *J. Solid State Chem.* **167**, 412 (2002).
- [9] O. Glemser and C. Naumann, *Z. anorg. allg. Chem.* **265**, 288 (1951).
- [10] A. Georg, W. Graf, and V. Wittwer, *Sol. En. Mat. Sol. Cells* **51**, 353 (1998).
- [11] J. Booth, T. Ekstroem, E. Iguichi, and R. Tilley, *J. Solid State Chem.* **41**, 293 (1982).
- [12] O. Glemser and H. Sauer, *Z. anorg. Chem.* **252**, 144 (1943).
- [13] M. Sienko and T. Truong, *J. Am. Chem. Soc.* **83**, 3939 (1961).
- [14] B. Brown and E. Banks, *J. Am. Chem. Soc.* **76**, 963 (1954).
- [15] W. Gardner and G. Danielson, *Phys. Rev.* **93**, 46 (1954).
- [16] M. Straumanis, *J. Am. Chem. Soc.* **71**, 679 (1949).
- [17] K.-S. Ahn, Y.-C. Nah, Y.-E. Sung, K.-Y. Cho, S.-S. Shin, and J.-K. Park, *Appl. Phys. Lett.* **81**, 3930 (2002).
- [18] R. Goldner, T. Haas, G. Seward, K. Wong, P. Norton, G. Foley, G. Berera, G. Wei, S. Schulz, and R. Chapman, *Solid State Ionics* **28-30**, 1715 (1998).
- [19] K. Bange, *Sol. En. Mat. Sol. Cells* **58**, 1 (1999).
- [20] J. Szymanski and A. Roberts, *Can. Mineral.* **22**, 681 (1984).
- [21] B. Krebs, *Acta Cryst. B* **28**, 2222 (1972).
- [22] M. Daniel, B. Desbat, J. Lassegues, B. Gerand, and M. Figlarz, *J. Solid State Chem.* **67**, 235 (1987).
- [23] B. Yan, Y. Xu, N. Goh, and L. Chia, *Chem. Commun.* (2000).
- [24] J. Johnson, A. Jacobson, S. Rich, and J. Brody, *J. Am. Chem. Soc.* **103**, 5246 (1981).
- [25] S. Kikkawa and Y. Teng, *Solid State Ionics* **113-115**, 403 (1998).
- [26] S. Ayyappan, G. Subbanna, and C. Rao, *Chem. Eur. J.* **1**, 165 (1995).
- [27] S. Chong, B. Ingham, and J. Tallon, *Curr. Appl. Phys.* **4**, 197 (2004).
- [28] B. Ingham, S. Chong, and J. Tallon, *Mat. Res. Soc. Symp. Proc.* **775**, P6.31 (2003).
- [29] S.-H. Lee, H. Cheong, J.-G. Zhang, A. Mascarenhas, D. Benson, and S. Deb, *Appl. Phys. Lett.* **74**, 242 (1999).
- [30] S. Chong, B. Ingham, and J. Tallon, *unpublished results*.
- [31] F. Cotton and R. Wing, *Inorg. Chem.* **4**, 867 (1965).
- [32] R. Silverstein, G. Bassler, and T. Morrill, *Spectrometric Identification of Organic Compounds* (Wiley, New York, 1991), 5th ed.
- [33] L. Segal and F. Eggerton, *Appl. Spec.* **15**, 112 (1961).
- [34] L. Segal, *Appl. Spec.* **17**, 21 (1963).
- [35] M. Baldwin, *Spectrochim. Acta* **18**, 1455 (1962).
- [36] A. Sabatini and S. Califano, *Spectrochim. Acta* **16** (1960).
- [37] D. Linde, ed., *CRC Handbook of Chemistry and Physics* (CRC Press, Boca Raton, 2000), 81st ed.
- [38] J. Brauman, J. Riveros, and L. Blair, *J. Am. Chem. Soc.* **93**, 3914 (1971).
- [39] E. Arnett, F. Jones, M. Taagepera, W. Henderson, J. Beauchamp, D. Holtz, and R. Taft, *J. Am. Chem. Soc.* **94**, 4724 (1972).
- [40] D. Aue, H. Webb, and M. Bowers, *J. Am. Chem. Soc.* **94**, 4726 (1972).
- [41] Commercial WO_3 powder is a pale yellow colour, which is reduced over 1-2 days in air to a pale green colour. This is indicative of a loss of oxygen but can be regained by storing in an oxygen atmosphere or heating in oxygen for a few hours.